Experimental testing of high capacity screwed and nailed connections in Douglas-fir CLT

Authors: Minghao Li, Justin Brown and Wenchen Dong

Date: 11th June 2020

Publication No: T098

TABLE OF CONTENTS

Disclaimer

supported by forestgrowers commodity levy

FOREST GROWERS RESEARCH

EXECUTIVE SUMMARY

This report presents experimental results of two project tasks. The first task is to study withdrawal behaviour of self-tapping screws (STS) in Douglas-fir CLT by conducting 167 withdrawal tests. It is very common to install STS with inclined angles to transfer shear loads between CLT panels in CLT buildings. Thus the screw withdrawal behavior needs to be well understood as it may govern the connection strength and stiffness. The second task is to study the ductility and overstrength properties of nailed hold-down connections in Douglas-fir CLT by conducting 40 hold-down connection tests. Nailed CLT hold-downs are commonly used in CLT shear wall structures to resist seismic loads. Ductility and overstrength properties of the hold-down connections are critical to achieve robust seismic design of CLT shear walls.

The experimental results demonstrated generally excellent connection behaviour in Douglas-fir CLT and the research outcome will provide valuable technical information for engineers to specific Douglas-fir CLT in building design.

TASK 1: WITHDRAWAL TESTS OF SELF-TAPPING SCREWS IN DOUGLAS-FIR CLT

Introduction

Self-tapping screws (STS) are the most popular fastener type used in CLT construction, in part due to their ease of installation and flexibility in design. For common wood screws and coach screws, New Zealand Timber Structures Standard NZS 3603 (Standards New Zealand, 1993) and Australian Timber Structures Standard AS 1720.1 (Standards Australia, 2010) provide tabular values for characteristic withdrawal capacity per millimetre of thread penetration for each timber species group. The recently proposed draft standard DZ NZS AS 1720.1 (2019) to supersede NZS 3603 only covers wood screws with Ø6.3mm or less. Therefore, design methods for the withdrawal capacity of STS are not covered by any of these standards.

Eurocode 5 (2014), Spax ETA (2017), and Ringhofer et al. (2015) provide methods for determining the withdrawal capacity of screws in solid and laminated timber products. EN 1382 (2016) specifies the formulation of the withdrawal parameter, f_1 in Eq. (1), to determine the fastener withdrawal capacity, F_{ax}. The key STS parameters to determine F_{ax} are shown in Figure 1. Following recent work by Ringhofer et al. (2018), the results presented herein are for the withdrawal strength prediction f_{ax}, defined in Eq. (2)

$$f_1 = \frac{F_{ax,max}}{l_{ef} d} \quad \left(\frac{N}{mm^2}\right) \qquad \text{Eq.(1)}$$

$$f_{ax} = \frac{f_1}{\pi} \quad \left(\frac{N}{mm^2}\right) \qquad \text{Eq.(2)}$$

$$l_{ef} = l_{nom} - d \qquad \text{Eq.(3)}$$

where d is the screw diameter; l_{nom} is the nominal screw installation length; l_{ef} is the effective thread embedment length excluding the length of the screw tip; and l_{emb} is the embedment length of unthreaded portion for a partially threaded screw.

Spax ETA (2017) and the method presented by Ringhofer et al. (2015) do not include l_{ef} in the calculation of f_1 whereas Eurocode 5 (2014) includes l_{ef} as an influencing parameter. Further, Eurocode 5 (2014), Spax ETA (2017), and Uibel and Blaß (2007) consider the screw tip length, l_{tip}, within l_{ef} for the calculation of f_1, whereas the Ringhofer et al. (2015) and the proposed draft DZ NZS AS 1720.1/V6 (2019) specifically state to neglect l_{tip} in the calculation of f_1 or l_{ef}. While the current NZS 3603 (Standards New Zealand, 1993) and AS 1720.1 (Standards Australia, 2010) do not explicitly feature STS withdrawal equations, design tables based on the joint group provide the characteristic capacity per millimetre penetration of the threaded portion for wood and coach screws. It is not clear if l_{tip} is considered or not. The embedment length of unthreaded portion, l_{emb} shown in Figure 1, is not considered as an influencing parameter in any design equations. This study will focus on the experimental derivation of the characteristic withdrawal strength of STS in Douglas-fir CLT.

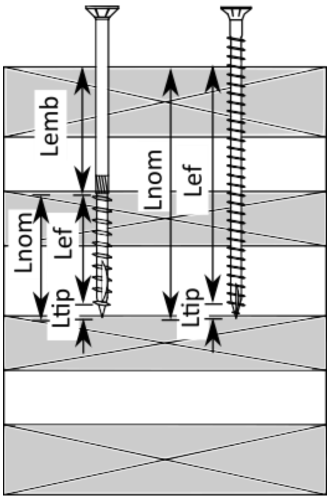

Figure 1: STS key parameters (partially threaded vs. fully threaded)

In this task, the withdrawal strength of STS in New Zealand Douglas-fir CLT by experimental testing is determined and the test results are compared to the screw design equations in literature, which have generally been derived from European softwood species which typically have lower density than New Zealand grown Douglas-fir.

Test programme

A total of 167 screw withdrawal tests were performed using Ø8mm and Ø12mm SPAX Delta Seal flat countersunk head screws. The tests considered varied Douglas-fir CLT layups, CLT installation faces, fastener diameters, screw installation angles (α+β). Generally, five to six replicates were performed at each of the 8d, 10d, 12d, and 16d nominal installation lengths, l_{nom}. With reference to Figure 1, l_{nom}=8d resulted in l_{ef}=56mm (excluding the screw tip of 1d) for a Ø8mm STS. The full experimental test programme is outlined in Table 1.

The CLT specimens were fabricated by XLAM Ltd. The Douglas-fir lamella were graded SG8 with average Modulus of Elasticity of 8 GPa according to NZS3603 (Standards New Zealand, 1993). The CLT specimens tested were 3-layer (CLT3) 5-layer (CLT5) and 7-layer (CLT7) as shown in Figure 2. The STS were installed on either the wide face or narrow face of CLT. Figure 3 shows the screw installation angles and possible screw location in the CLT wide or narrow face. The primary thread-grain angle α is shown as per Figure 3 and the secondary angle β is out-of-plane of the primary wood grain direction. In this testing programme, screws installed in the CLT narrow face were only installed in position 4. In some instances, a compound α°+β° angle was used. The CLT specimens had an average moisture content of 11% and the mean density ρ_m and the characteristic density ρ_k are provided in Table 2.

Table 1: STS withdrawal test matrix

Test ID	CLT Type	CLT Installation Face	Screw Diameter, Ø (mm)	Angle to grain (α°+β°)	Number of tests at each l_{nom}			
					8d	10d	12d	16d
CLT3-8-90	CLT3	Wide	8	90	5	5	5	5
CLT5-8-90	CLT5		8	90	6	5	6	5
CLT5-8-60			8	60	5	5	5	-
CLT5-8-60+15			8	60+15	5	5	-	-
CLT5-8-0		Narrow	8	0	5	5	5	1
CLT5-8-30			8	30	8	5	6	-
CLT5-8-30+15			8	30+15	5	5	5	-
CLT7-12-90	CLT7	Wide	12	90	5	5	5	5
CLT7-12-60			12	30	5	5	-	-
CLT7-12-0		Narrow	12	0	5	5	-	-
CLT7-8-0			8	0	-	-	5	5

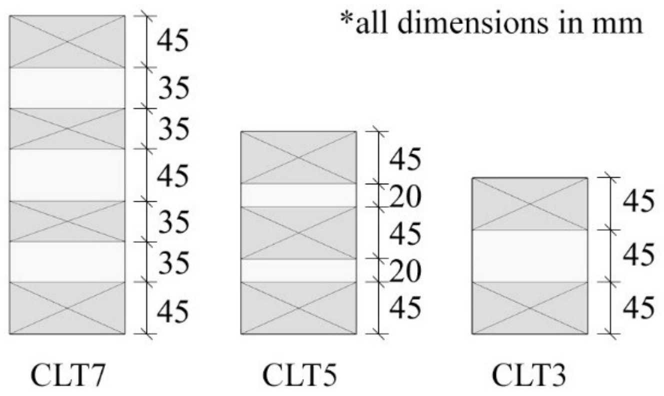

Figure 2: CLT types used in test programme

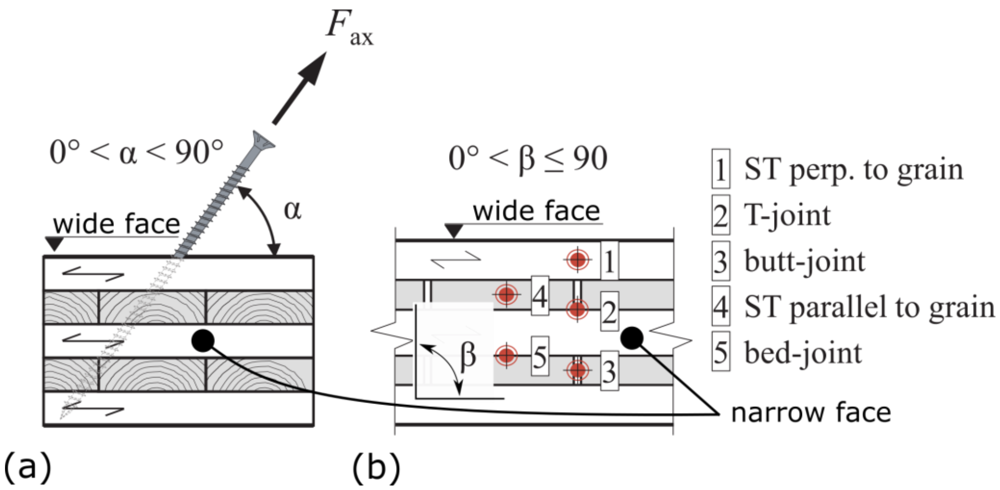

Figure 3: Screw installation angle: (a) relative to outer wood grain and (b) possible positions in CLT narrow face. Adopted from (Ringhofer et al., 2018)

Table 2: CLT specimen and individual layer density (kg/m3)

	CLT3	CLT5			CLT7	
Sample	Specimen	Specimen	45mm lamella	20mm lamella	Specimen	35mm lamella
ρ_m(kg/m^3)	478.4	463.7	461.8	538.6	457.4	464.5
ρ_k(kg/m^3)	426.4	421.8	413.3	487.3	416.5	420.5

All tests were performed in displacement control following EN 1382 (2016). The test set-up for the 90° and inclined screw withdrawal tests are shown in Figure 4 and Figure 5.

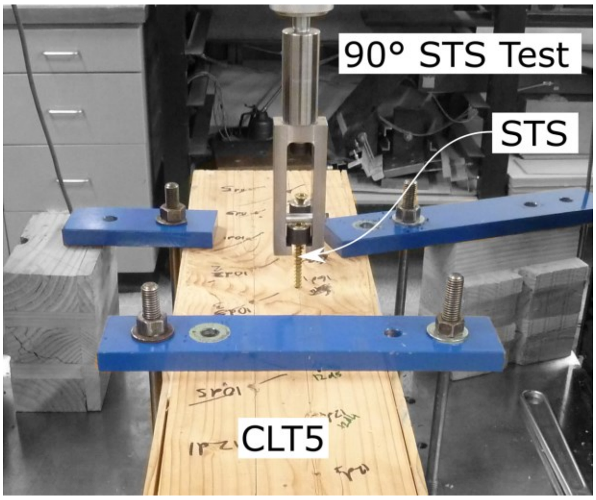

Figure 4: 90 degree screw withdrawal test setup

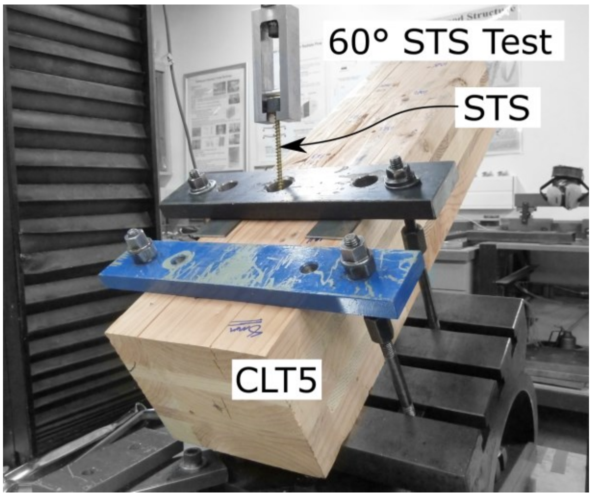

Figure 5: Inclined screw withdrawal test setup

Results and discussion

Figure 6 shows the summary of the withdrawal strength for each test series. The experimental results combine the l_{nom} tests of 8d, 10d and 12d assuming l_{ef} is not an influencing parameter on withdrawal strength as per Ringhofer et al. (2015). As expected, the withdrawal strength was higher for the ø8mm series compared to the ø12mm screw series. Further, an increasing strength and homogenization was observed with increasing number of CLT layers penetrated. Withdrawal strengths for the CLT5 test series on the narrow face, which included the installation angles of 0°, 30°, and 30°+15°, had high strength but also high variability. This higher withdrawal strength is in part due to the higher density of the 20mm lamella layer as reported in Table 2.The compound installation angle (α+β) on the CLT narrow face had a lower coefficient of variation (CV) when compared to the single angle. Therefore, engaging more CLT layers with a compound angle installation increased homogenization. However, the withdrawal strength of the compound angle was lower than the single angle test results. The benefit of lower dispersion was not observed in compound angle withdrawal tests on the CLT wide face.

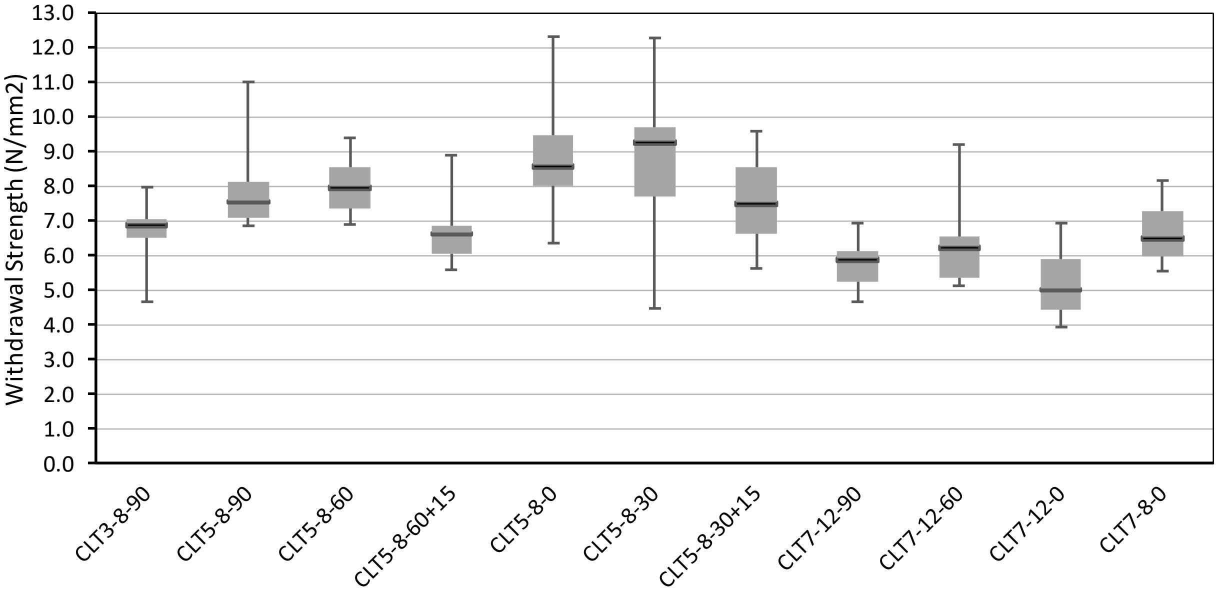

Figure 6: Withdrawal strength of various test series

In all test series, the 16d embedment length reached the steel tensile capacity of the screws. In this instance, the characteristic steel tensile results were determined as per EN 14358 (2016). Table provides a comparison of the experimental results to the Spax ETA (2017) characteristic tensile values.

Table 3: Tensile capacity of screw with comparison to ETA

Screw	$F_{tens,ETA,k}$ (kN)	$F_{tens,exp,k}$ (kN)	$F_{tens,exp,mean}$ (kN)	Sample size
Ø8mm	17	19.2	21.4	16
Ø12mm	38	41.8	49.0	3

Typical failure modes in the CLT wide face and CLT narrow face testing are shown in Figure 7 and Figure 8.

Figure 7: Timber splitting in CLT wide face 90° screw withdrawal test

Figure 8: Shear cylinder failure in CLT narrow face 0° screw withdrawal test

Table 4 compares the characteristic withdrawal strength with the calculations by the ETA and Ringhofer analytical methods. The ETA and Ringhofer methods were compared because they do not include l_{ef} as an influencing parameter on f_{ax}. In general, there is good agreement between the analytical methods and the experimental results given the relatively small sample size of each test series. The higher characteristic withdrawal strength predicted by the Ringhofer method when compared to ETA is in part due to the higher density correction factor used by Ringhofer. The experimental results of the narrow face 0° installation are significantly higher than the analytical methods. With reference to Figure 3, this result is expected as all experimental tests were installed in location 4 (screws driven in end grain) whereas both ETA and Ringhofer methods account for all possible installation locations. If a screw was installed in location 3 the withdrawal strength would be lower.

Table 4: Comparison of full experimental characteristic withdrawal strength, fax,k,i (N/mm2)

Test ID	CLT3-8-90	CLT5-8-90	CLT5-8-60	CLT5-8-60+15	CLT5-8-0	CLT5-8-30	CLT5-8-30+15	CLT 7-12-90	CLT 7-12-60	CLT 7-12-0	CLT 7-8-0
$f_{ax,k,exp}$	5.2	5.9	6.6	4.9	5.9	5.3	5.5	4.6	4.2	3.4	4.9

CV_{exp}(%)	12.2	16.6	9.6	15.2	18.5	21.5	15.4	11.2	20.0	19.2	14.2
$f_{ax,k,ETA}$	4.5	4.4	4.2	4.2	4.1	4.3	4.3	4.0	3.8	3.4	3.7
$f_{ax,k,Ringhofer}$	6.0	5.9	5.9	5.9	3.3	5.4	5.4	5.1	5.1	2.5	2.9

Figure 9 shows the comparison between seven analytical design methods found in literature or building codes, fax,i, and the characteristic withdrawal strength of the test series CLT3-8-90 and CLT7-12-90. Most methods in literature under-predicted the withdrawal strength except for the Ringhofer method. The Uibel and Blasß (U&B) (2007), Eurocode 5 (EC5) (2014), and the SPAX ETA (ETA) (2017) equations all provide similar strength predictions with the inclusion of l_{tip} having a larger impact on the ø12mm screw size for U&B and EC5. It should be pointed out that NZS3603 and AS 1720.1 tabular values and the proposed design method in DZ NZS AS 1720.1/V6.0 all for coach screws were used and they are not representative of STS as expected.

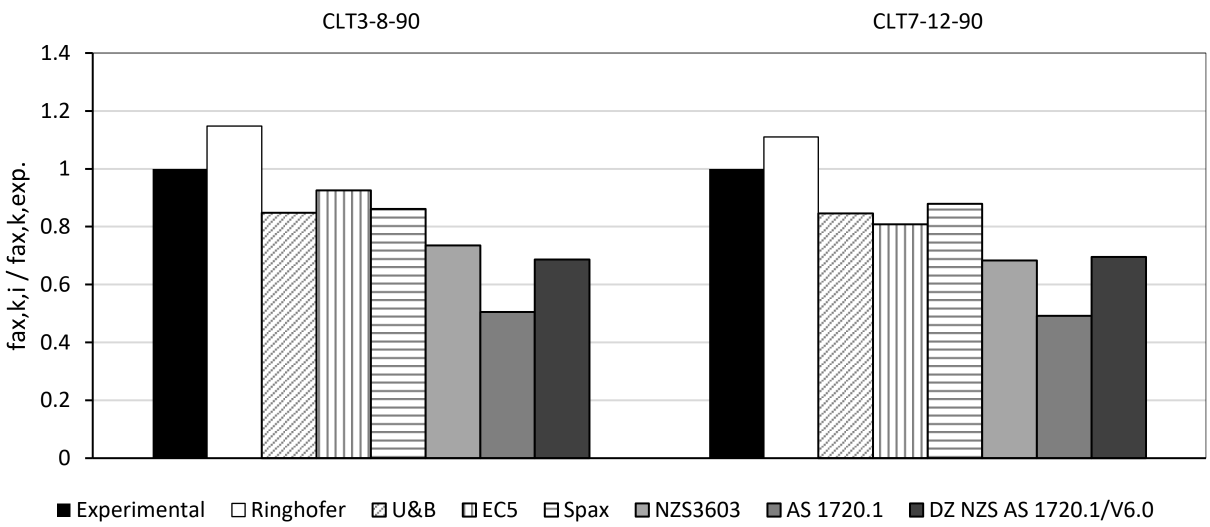

Figure 9: Comparison of characteristic withdrawal strength according to experimental results for ø8mm and ø12mm screws at constant 10d length and 90° installation

Conclusions

A total of 167 STS withdrawal tests of ø8mm and ø12mm screws in three-, five- and seven-layer Douglas-fir CLT were performed. Experimental results were compared with seven analytical design methods in literature.

To avoid brittle steel tensile failure of STS, embedment length of the threaded portion should not be greater than 12d. The experimental results showed that Eurocode 5 (2014), Spax ETA (2017), Uibel and Blaß (2007), and Ringhofer et al. (2015) analytical design equations were generally applicable for the STS in Douglas-fir CLT within a 15% prediction error for the characteristic withdrawal strength.

It was also found that the experimental withdrawal strength from CLT narrow face installation generally was higher than the predictions. However, our study only considered one screw installation location without considering all possible installation locations on the narrow surface. While the current NZS 3603 (Standards New Zealand, 1993), AS 1720.1 (Standards Australia, 2010) do not specify STS, using their design values for coach screws could significantly under-predict the withdrawal strength of STS. The proposed DZ NZS AS 1720.1/V6 (2019) analytical equation for screws with Ø6.3mm or less and coach screws also significantly under-predicted the withdrawal strength.

TASK 2: NAILED HOLD-DOWN CONNECTION TESTS IN DOUGLAS-FIR CLT

2.1 Introduction

Wall-to-foundation anchoring connection systems have critical contributions to lateral resistance of CLT structures under wind or seismic loads. Utilization of nails along with steel brackets for hold-down connections and shear keys is a common practice. Nailed hold-down connections are used to provide uplifting restraints for CLT shear walls under seismic loads. Their performance has a direct relationship with the number and the type of nails used to connect the hold-down brackets to CLT panels. Ductile failure characterized by yielding of nails was observed when hold-down connections had nail quantities less than half the number of the pre-drilled holes on the commercial brackets (Flatscher et al. 2015, Benedetti et al. 2019). However, the effect of nailing pattern on failure mechanisms of hold-down connection systems has not been researched.

This study is to assess the structural performance of nailed hold-down connections in Douglas-fir CLT. Influence of hold-down design parameters including nailing patterns, nail length, timber species, and hold-down bracket types on the hold-down connection performance including ductility and overstrength is investigated. The test results will provide insightful information for robust seismic design of Douglas-fir CLT shear walls following the capacity design approach.

2.2 Test programme

Table 5 lists the test matrix of the hold-down connections. A total of 40 connection specimens were constructed by installing commercial WHT440 hold-down brackets (Rothoblaas, 2019) on Douglas-fir CLT. WHT440 bracket is one of the common hold-down brackets used in CLT construction to provide overturning restraints to shear walls under lateral loads; it is composed of 3 mm thick steel plates with thirty ø5 mm holes. Four different hold-down types were defined to include three nailing patterns and two nail sizes as experimental design factors. For example, “F”-ø4×60 type represents hold-down connections with ø4×60 nails in a full nailing pattern “F”. Table 6 lists the properties of the CLT materials in terms of layups, timber grades, densities, and moisture contents. The characteristic densities were calculated according to EN 14358 (2016). These characteristic densities were used in the calculation of the characteristic strength of the hold-down connections.

The nails were driven through the holes of the brackets following the patterns illustrated in Figure 10: full nailing (“F”) and two partial nailing (“P1” and “P2”) patterns.

Table 5: Test matrix of hold-down connections

Hold-down type		Nail size			No. of replicates

	Bracket type		Nail quantity	Nailing pattern[1]	Mono.	Cyc.
“F”-ø4×60	WHT440	ø4×60	30	F	5	5
“P1”-ø4×60		ø4×60	15	P1	5	5
“P1”-ø4×50		ø4×50	15	P1	5	5
“P2”-ø4×50		ø4×50	15	P2	5	5

Note: 1. nailing patterns are shown in Figure 1 and Figure 2.

Table 6: Summary of CLT properties

CLT layup	Timber grade	Density (kg/m^3)		Moisture content
		ρ_{mean}	ρ_k	mean
35/35/35	SG8	467	421	10.9%

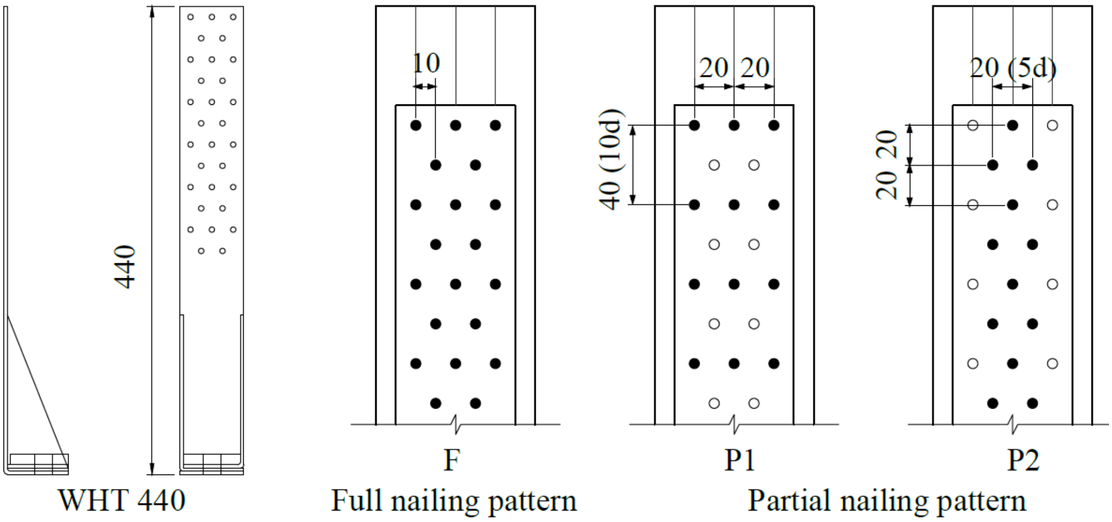

Figure 10: WHT440 bracket and nailing patterns in Type A and Type B hold-down connections

As shown in Fig. 11, CLT blocks were restrained by steel rods and steel plates in place, while the load was applied by an actuator connected to the hold-down bracket via a ø16 mm anchoring bolt. One potentiometer was mounted onto the specimens to measure the relative displacement/slip between the hold-down bracket and the CLT along the vertical loading direction.

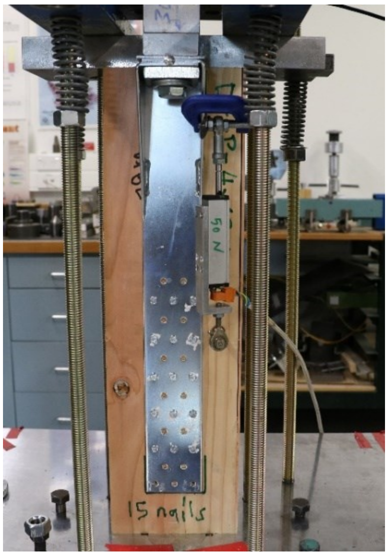

Figure 11: Experimental set up

As shown in Table 5, five replicates of each hold-down sub-type were tested under each monotonic and cyclic loading condition. For the monotonic tests, the displacement controlled loading rate of 2-3 mm/min was implemented. For the cyclic tests, the CUREE protocol proposed by Krawinkler et al. (2000) was implemented. Excursions of positive displacements were applied to the hold-down specimens to simulate the seismic excitations, as shown in Figure 12. The amplitudes of the loading cycles were determined based on the displacements correspond to the post-peak loads equivalent to 80% of the peak loads obtained from the monotonic tests. The cyclic loads were applied at a constant rate of 10 mm/min.

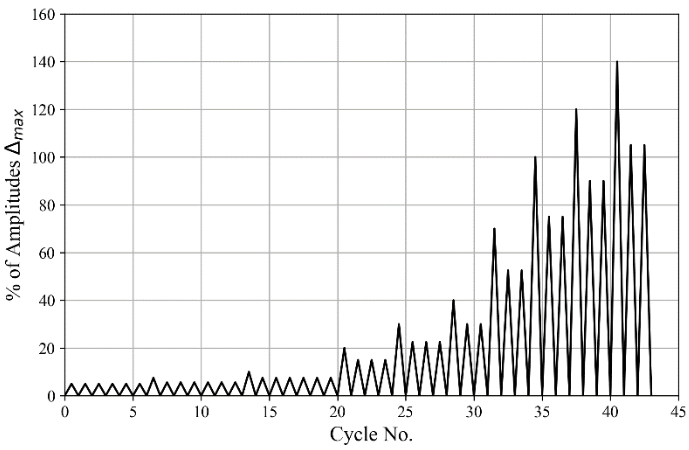

Figure 12: CUREE loading protocol

2.3 Results and discussion

Failure Modes

The dominant failure mode of the hold-down connections with the full nailing pattern “F” was the hold-down bracket fracture, as shown in Figure 13a. The tensile fracture of the brackets generally occurred at their top nail rows which were responsible for carrying higher loads than other rows of nails. Also due to the loading eccentricity, the brackets were deformed out-of-plane as shown in Figure 13b. The combination of high tensile stresses and bending stresses at the reduced cross sections of the brackets ultimately led to the fracture failure. These observations suggested that such a failure mode can reduce the connection ductility and energy dissipation, while it suppresses the ductile behaviour of the nails.

The hold-down connections with the partial nailing patterns failed due to nail withdrawal and nail head shear-off (shown in Figure 14a) together with bracket bending (shown in Figure 14b). As the number of nails was reduced by half from the full nailing pattern, the hold-down connection performance was governed by the behaviour of the nails. In general, ductile nail behaviour characterized by severe bending of its shank and wood embedment crushing was observed, which eventually led to nail withdrawal failure. Interestingly, under the monotonic loading, nail head shear-off occurred in a large number of nails in combination with the withdrawal failure. However, it was not typically observed for the same connections under cyclic loading. A possible explanation for this phenomenon is that the cyclic loading can gradually withdraw the nails and the locations of plastic hinges along the nail shanks may slightly shift during the cyclic tests.

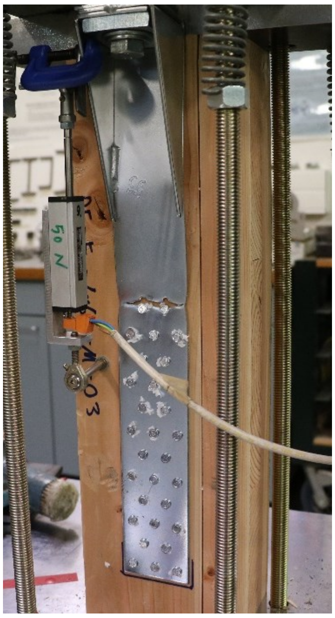
(a)


(b)

Figure13 Typical failure modes in hold-down connections with full nailing pattern “F”: (a) Bracket fracture, and (b) Bracket bending deformation

 

(a) (b)

Figure 14 Typical failure modes in hold-down connections with partial nailing patterns: (a) Nail withdrawal and head shear-off, and (b) bracket bending deformation

Hold-down connection properties

It was found that the curves in each hold-down type were consistent. Therefore, for each hold-down type, one representative monotonic load-slip curve and one representative cyclic load-slip curve are provided in Figure 15. In general, the backbones of the cyclic curves matched well against the monotonic curves. Table 7 list the derived connection properties based on the load-slip curves following the EEEP approach in ASTM E2126 (2011). The variability in each connection type was primarily due to the inherent variability of wood including inconsistent density, moisture contents, grain direction, natural defects, etc.

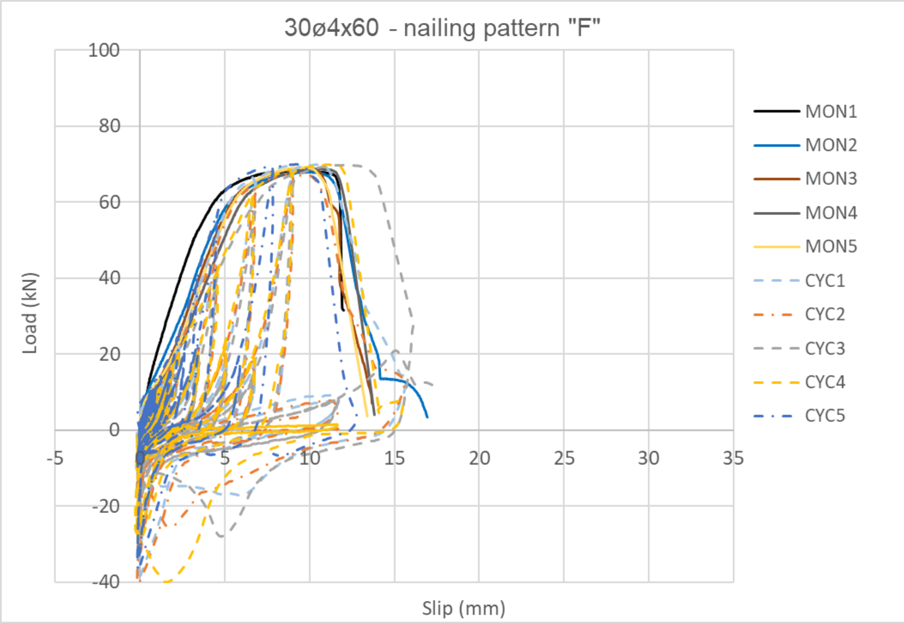
30ø4x60 - nailing pattern "F"
Load (kN)
Slip (mm)
MON1
MON2
MON3
MON4
MON5
CYC1
CYC2
CYC3
CYC4
CYC5

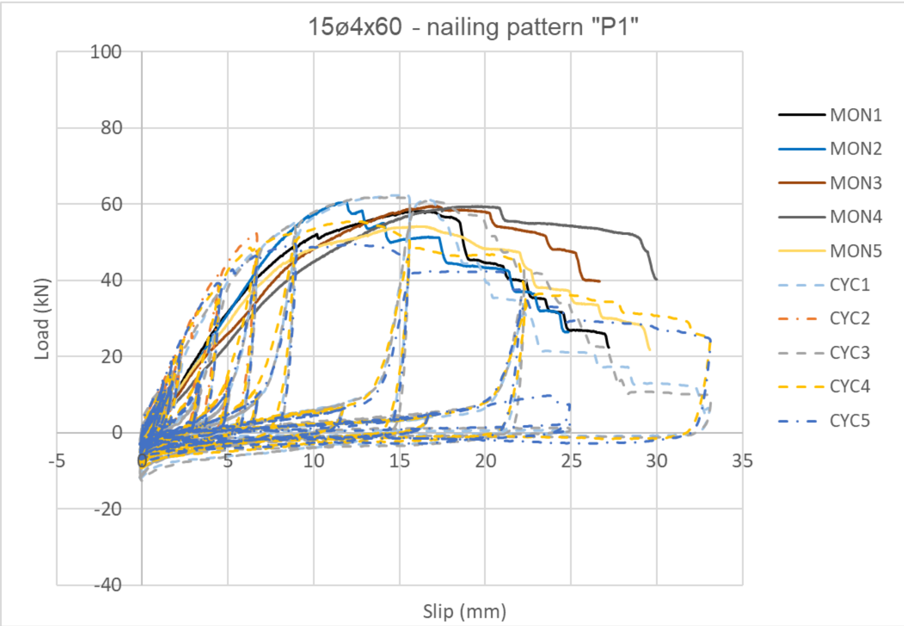
15ø4x60 - nailing pattern "P1"
Load (kN)
Slip (mm)
MON1
MON2
MON3
MON4
MON5
CYC1
CYC2
CYC3
CYC4
CYC5

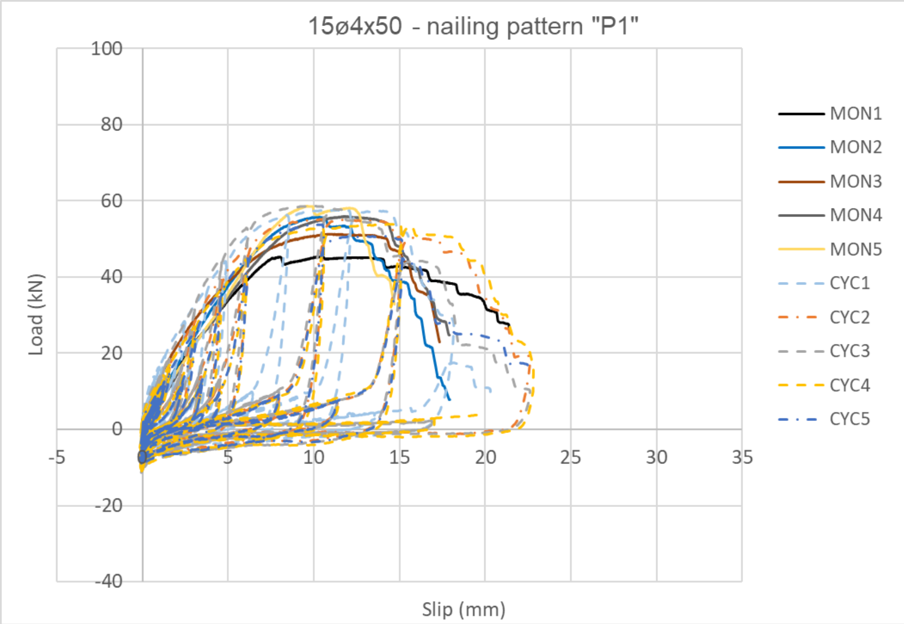

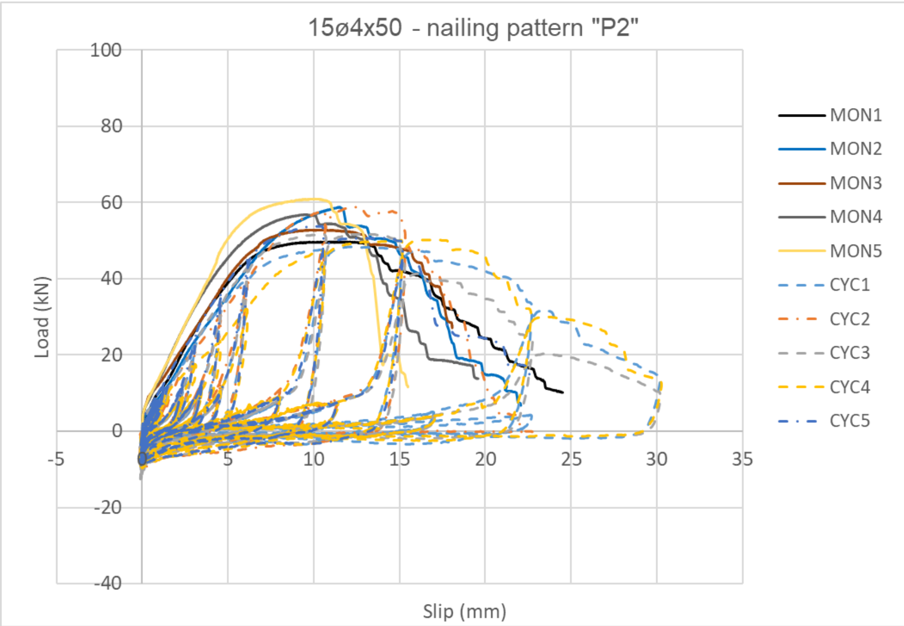

Figure 15 Load-slip curves of hold-down connections

The hold-down strength predictions followed Eurocode 5 (2004) except for the “F”-ø4x60 hold-down connections as their governing failure mode was the steel bracket failure. Although 3 mm thick WHT440 bracket was between thin and thick plates compared with the nail diameter 4 mm, the condition of thick plate was satisfied due to the use of the conical-shaped cap, annular-ringed shank nails (Izzi et al. 2016). Equation (4) from Eurocode 5 was used to calculate the load-carrying capacities for the hold-downs when nail failure governed their failure mode. It considers three possible failure modes: failure solely by embedment in the timber; failure by a combination of embedment in the timber and single yielding in the fastener; and failure by a combination of embedment in the timber and double yielding in the fastener. Equation (5) from the CLT Handbook was used to estimate the CLT embedment strength. For “F”-ø4x60 hold-down connections, the manufacturer specified bracket tensile strength was provide as the predicted hold-down strength.

$$F_k = \min \begin{cases} n_1 n_2 f_{h,k} t_1 d \\ n_1 n_2 f_{h,k} t_1 d \left[\sqrt{2 + \frac{4M_{y,Rk}}{f_{h.k} d t_1^2}} - 1\right] + \frac{F_{ax.Rk}}{4} \\ n_1 n_2 2.3\sqrt{2M_{y,Rk} f_{h.k} d} + \frac{F_{ax.Rk}}{4} \end{cases} \quad \text{Eq. (4)}$$

$$f_{h,k} = 0.112 d^{-0.5} \rho_k^{1.05} \quad \text{Eq. (5)}$$

where, F_k = characteristic value of hold-down strength; n_1, n_2 = the row and column number of nails in the hold-down connection; $f_{h,k}$ = the characteristic embedment strength in the timber member; t_1 = the nail penetration depth; d = the nail diameter; $M_{y,Rk}$ = the characteristic nail yield moment (6500 N·mm for ø4x50 and ø4x60 according to manufacturer information and 8822 N·mm for ø4x100 according to bending test); $F_{ax,Rk}$ = the characteristic withdrawal capacity of nails calculated according to Eurocode 5; ρ_k = the characteristic density of timber.

To calculate the fastener group characteristic strength, the actual fastener quantity was used instead of the effective fastener number n_{eff} provided in Eurocode 5, as recommended by previous research from Ottenhaus et al. (2018b).

The overstrength factors of individual hold-down connections $\gamma_{Rd,i}$ and the hold-down group γ_{Rd} were calculated by Equation (6) and Equation (7), respectively. $F_{0.95}$ for each hold-down group was calculated according to EN 14358 assuming the data were normally distributed.

$$\gamma_{Rd,i} = \frac{F_y}{F_k} \quad \text{Eq. (6)}$$

$$\gamma_{Rd} = \frac{F_{0.95}}{F_k} \quad \text{Eq. (7)}$$

Table 7: Summary of hold-down connection test results

Hold-down sub-type		F_k[1] (kN)	F_y (kN)	Δ_y (mm)	F_{max} (kN)	Δ_{max} (mm)	F_u (kN)	Δ_u (mm)	K (kN/mm)	μ	$\gamma_{Rd,i}$	γ_{Rd}
“F”-ø4x60	M1	63.4[1]	65.0	4.6	68.2	8.7	54.5	12.4	13.5	2.6	n/a	n/a
	M2		65.7	5.2	68.1	9.8	54.4	12.1	12.6	2.3		
	M3		67.7	6.2	69	10.1	55.2	11.7	11.0	1.9		
	M4		70.0	7.4	68.8	10.5	55.1	12.3	9.5	1.7		
	M5		70.4	6.9	69.2	9.8	55.4	11.4	10.2	1.7		
	M_{avg}		*67.8*	*6.1*	*68.7*	*9.8*	*54.9*	*11.9*	*11.4*	*2.0*		
	C1		71.2	7.1	69.2	10.6	55.9	12.1	10.0	1.7		
	C2		68.5	7.1	67.5	8.9	54.0	11.3	9.7	1.6		

	C3		68.4	8.1	69.9	12.3	55.9	14.6	8.5	1.8		
	C4		69.5	7.7	68.8	11.2	55.9	12.5	9.0	1.6		
	C5		71.8	6.4	70.0	9.3	56.0	10.9	11.2	1.7		
	C_{avg}		*69.9*	*7.3*	*69.1*	*10.4*	*55.5*	*12.3*	*9.7*	*1.7*		
	Avg-All		68.8	6.6	68.9	10.1	55.2	12.1	10.6	1.9		
	M1		53.8	8.5	58.1	16.7	46.5	18.9	6.4	2.2	1.42	
	M2		55.3	9.0	60.5	11.9	48.4	17.4	6.1	1.9	1.46	
	M3		55.0	10.3	59.5	17.2	47.6	25.1	5.3	2.4	1.45	
	M4		55.6	11.8	59.5	19.8	47.6	29.5	4.7	2.5	1.47	
	M5		50.5	8.8	54.2	16	43.4	22.4	5.8	2.5	1.34	
	M_{avg}		*54.1*	*9.7*	*58.4*	*16.3*	*46.7*	*22.7*	*5.7*	*2.3*		
“P1”-ø4x60	C1	37.8	57.6	7.0	62.6	15.5	50.1	18.2	8.2	2.6	1.52	1.62
	C2		52.3	4.9	56.7	10.7	45.4	15.3	10.6	3.1	1.38	
	C3		56.8	6.4	61.8	14.9	49.4	20.8	8.9	3.3	1.50	
	C4		49.7	4.9	55.4	12.8	44.3	22.0	10.1	4.4	1.31	
	C5		45.2	4.1	49.7	8.9	39.7	21.4	10.9	5.1	1.20	
	C_{avg}		*52.3*	*5.5*	*57.2*	*12.6*	*45.8*	*19.5*	*9.7*	*3.7*		
	Avg-All		53.2	7.6	57.8	14.5	46.2	21.1	7.7	3.0		
	M1		42.6	5.5	45.4	10.4	36.3	18.4	7.7	3.3	1.16	
	M2		51.4	6.3	55.8	10.3	44.6	13.7	8.1	2.2	1.40	
	M3		46.9	4.2	51.2	11.7	41	15.7	11.2	3.8	1.28	
	M4		52.1	7.0	55.9	12.0	44.7	15.5	7.5	2.2	1.42	
	M5		56.6	7.8	58.7	9.6	46.9	13.2	7.3	1.7	1.54	
	M_{avg}		*49.9*	*6.2*	*53.4*	*10.8*	*42.7*	*15.3*	*8.4*	*2.6*		
“P1”-ø4x50	C1	36.7	52.8	3.9	57.6	11.6	46.1	15.7	13.6	4.0	1.44	1.61
	C2		51.0	5.1	55.1	10.5	44.1	19.0	10.1	3.8	1.39	
	C3		54.4	4.6	58.7	10.1	46.9	14.3	11.9	3.1	1.48	
	C4		49.8	5.1	54.1	15.0	43.3	19.8	9.8	3.9	1.36	
	C5		49.0	5.4	53.8	10.1	43.1	16.2	9.0	3.0	1.34	
	C_{avg}		*51.4*	*4.8*	*55.9*	*11.5*	*44.7*	*17*	*10.9*	*3.6*		
	Avg-All		50.7	5.5	54.6	11.1	43.7	16.1	9.6	3.1		
	M1		46.4	5.2	49.7	12.4	39.7	16.6	8.9	3.2	1.26	
	M2		52.7	6.8	58.8	11.6	47	15	7.7	2.2	1.44	
	M3		49.5	5.2	52.8	11.1	42.2	16.4	9.4	3.1	1.35	
“P2”-ø4x50	M4	36.7	51.8	4.4	56.8	9.6	45.5	13.7	11.9	3.1	1.41	1.58
	M5		57.2	5.0	61.0	10.0	48.8	13.0	11.5	2.6	1.56	
	M_{avg}		*51.5*	*5.3*	*55.8*	*10.9*	*44.7*	*14.9*	*9.9*	*2.9*		
	C1		45.1	6.1	48.4	12.6	38.7	21.8	7.4	3.6	1.23	
	C2		54.2	7.9	58.9	12.7	47.1	16.4	6.8	2.1	1.48	

C3	49.5	6.8	51.6	13.6	41.3	16.4	7.2	2.4	1.35
C4	48	8.8	50.2	17.4	40.2	20.7	5.4	2.3	1.31
C5	50.2	8.7	53.2	15.1	42.6	19.6	5.8	2.3	1.37
C_{avg}	*49.4*	*7.7*	*52.5*	*14.3*	*42.0*	*19.0*	*6.5*	*2.5*	
Avg-All	50.5	6.5	54.1	12.6	43.3	17.0	8.2	2.7	

Note: 1. the hold-down strength prediction of “F”-ø4x60 is governed by hold-down bracket tensile capacity. Other types of hold-down strength predictions are governed by nail strength.

As shown in Table 7, the average yield strength of “F”-ø4x60 was 68.8 kN, similar with the characteristic tensile strength 63.4 kN of the WH440 bracket listed in the product specifications (Rothoblaas, 2019). Due to the brittle tensile failure of the bracket, the average ductility factor (μ) of 1.9 was achieved. Therefore, this hold-down system with full nailing pattern is not ideal to be used as a ductile element in CLT shear wall design, and its overstrength factor is not provided in the table. In “P1”-ø4x60 hold-down connections, the nail quantity was reduced by half from the full nailing pattern. This change in the nailing pattern increased the connections’ average ductility factor by 58% to 3.0, while it dropped the average yield strength by 23% from 68.8 kN to 53.2 kN. In “P1”-ø4x50 hold-down connections, the connection configuration was the same as “P1”-ø4x60 connections except that the nails were 10 mm shorter. The yield strength and the average μ of both hold-down types were similar (53.2 kN vs. 50.7 kN and 3.0 vs. 3.1). “P2”-ø4x50 hold-down connections had the same number of nails as P1”-ø4x50 hold-downs, but the nail spacing was reduced by half and the nailing pattern was staggered, as shown Figure 10. The change of the nailing pattern did not have an influence on the yield strength (50.5 kN vs. 50.7 kN), but reduced μ by 13% from 3.1 to 2.7. The overstrength factors γ_{Rd} of the hold-down connections with partial nailing patterns ranged from 1.58 to 1.62 with an average of 1.60, which was consistent with the range of overstrength factors of dowelled CLT hold-down connections derived by Ottenhaus et al. (2018b). The results of yield strength and ductility from the monotonic tests and cyclic tests were also compared for all hold-down connection sub-groups except for F”-ø4x60 what experiencing brittle bracket fracture failure. All hold-down connection types achieved the similar average yield strength values during the monotonic and cyclic tests.

2.4 Conclusions

An experimental study was conducted to investigate the structural performance of nailed Douglas-fir CLT hold-down connections for CLT shear walls. Hold-down connection properties including strength, stiffness, ductility and overstrength were derived. The influence of various design parameters on the hold-down behaviour was also studied. The main conclusions are provided as follows:

- The commercial WHT440 hold-down brackets with 15 ø4x50 or ø4x60 nails in the partial nailing patterns were able to provide connection ductility factors of μ=2.7-3.1 and connection overstrength factors of γ_{Rd} = 1.58-1.62. However, it is critical to avoid brittle tensile failure of the bracket which may cause low ductility of μ<2.0. The initial stiffness of hold-down connections with partial nailing patterns ranged from 7.7-9.6 kN/mm.
- In general, two nail lengths (ø4x50 vs. ø4x60) caused similar yield strength and ductility for the hold-down connections. Partial nailing patterns "P1" and "P2" had similar yield strength and overstrength γ_{Rd}.

REFERENCES

- ASTM E2126, 2011. Standard Test Methods for Cyclic (Reversed) Load Test for Shear Resistance of Vertical Elements of the Lateral Force Resisting Systems for Buildings, ASTM International.
- Benedetti, F., Rosales, V., Opazo-Vega, A., Norambuena-Contreras, J. and Jara-Cisterna, A., 2019. Experimental and numerical evaluation of hold-down connections on radiata pine Cross-Laminated-Timber shear walls: a case study in Chile. European Journal of Wood and Wood Products, 77(1): 79-92.
- CEN. (2014). Eurocode 5: Design of timber structures-Part 1-1: General-Common rules and rules for buildings. EN1995-1-1:2004-11 + AC2006-06 + A1:2008-06 + A2:2014-05 Eurocode 5. Brussels, Belgium: European Committee for Standardization.
- EN 1382. (2016). Timber structures - test methods - withdrawal capacity of timber fasteners. European Committee for Standardization (CEN).
- EN 14358, 2016. Timber structures –Calculation and verification of characteristic values. European Committee for Standardization, Bruxelles, Belgium.
- ETA. (2017). European technical approval: screws for use in timber constructions (ETA-12-011). Brussels, Belgium: European Organisation for Technical Approvals.
- Flatscher, G., Bratulic, K. and Schickhofer, G., 2015. Experimental tests on cross-laminated timber joints and walls. Proceedings of the Institution of Civil Engineers-Structures and Buildings, 168(11):868-877.
- Krawinkler, Parisi, F., Ibarra, L., Ayoub, A., and Medina, R. 2000. Development of a Testing Protocol for Wood Frame Structures. *CUREE Publication No. W-02*, Consortium of Universities for Research in Earthquake Engineering, CA, U.S.
- Izzi, M., Flatscher, G., Fragiacomo, M., & Schickhofer, G, 2016. Experimental investigations and design provisions of steel-to-timber joints with annular-ringed shank nails for Cross-Laminated Timber structures. Construction and Building Materials, 122, 446–457.
- NZS/AS 1720.1, 2019. Timber Structures Part 1: Design methods (draft for public consultation). Standards New Zealand, Wellington, New Zealand
- Ottenhaus, L., Li, M., Smith, T. and Quenneville, P. 2018. “Overstrength of dowelled CLT connections under monotonic and cyclic loading”, Bulletin of Earthquake Engineering. 16(2):753-773.
- Ringhofer, A, Brandner, R., & Schickhofer, G. (2015). 48-07-01 - A universal approach for withdrawal properties of self-tapping screws in solid timber and laminated timber products. INTER 2015, 79–96.
- Ringhofer, Andreas, Brandner, R., & Blaß, H. J. (2018). Cross laminated timber (CLT): Design approaches for dowel-type fasteners and connections. Engineering Structures.
- Rothoblaas, 2019. WHT Angle bracket for tensile loads. Rothoblaas design manual. Cortaccia, Italy.
- Standards Australia. (2010). AS 1720.1-2010 Timber Structures Part 1 Design Methods.pdf. Sydney, Australia: Standards Australia.
- Standards New Zealand. (1993). Timber structures standard (NZS 3603). Private Bag 2439, Wellington, New Zealand: Standards New Zealand,.

- Uibel, T., & Blaß, H. J. (2007). 40-7-2 - Edge joints with dowel type fasteners in cross laminated timber. Working Commission W18 - Timber Structures. Bled, Slovenia.